JAISCR, 2026, Vol. 16, No. 2, pp. 145 – 162
10.2478/jaiscr-2026-0008

COMMUNITY DETECTION WITH HIGHER-ORDER EDGE ENHANCEMENT IN TEMPORAL NETWORKS

Feiyu Yin[1], Yu Xia[2,*], Agnieszka Siwocha[3], Zhanyu Cen[4], Jie Chen[5,*]

[1]*College of Biomedical Engineering, Fudan university, Shanghai, 200438, China*

[2]*State Key Laboratory of Mechanical System and Vibration, Shanghai Jiao Tong University, Shanghai, 200240, China*

[3]*Information Technology Institute, SAN University, 90-113 Łódź, Poland*

[4]*Ningbo Zhongda Leader Intelligent Transmission Co., Ltd., Ningbo 315300, China*

[5]*College of Electronic Engineering, National University of Defense Technology, Changsha, 410073, China*

[*]*E-mail: rainyx@sjtu.edu.cn; jchen202209@163.com*

Submitted: 20th September 2025; Accepted: 27th December 2025

Abstract

Dynamic community detection often suffers from the instability of results, making consistent community identification across network snapshots critically important. However, the cut off between snapshots might lead to the loss of some higher-order structures, such as closed triangle motifs. In view of this, we examine the relationship between the missing higher-order structures and the instability, and find a positive correlation between higher-order loss ratio (HOLR) and temporal smoothing normalized mutual information (TS-NMI). Based on this finding, we propose a new-brand higher-order edge enhancement (HOEE) algorithm, aiming to effectively reconstruct higher-order interactions to overcome the instability issue. The HOEE algorithm employs the higher-order activity potential (HAP) of nodes between consecutive snapshots to recover the loss of higher-order information by the transformation of the triangle motif, thus ensuring the temporal stability of dynamic communities. Experimental evaluation on synthetic and real-world dynamic networks demonstrates that HOEE outperforms state-of-the-art methods in community detection accuracy and significantly reduces community instability. Theoretical analysis confirms stability guarantees and characterizes graph property changes induced by HOEE. The HOEE algorithm effectively enhances temporal community stability through higher-order interaction reconstruction, providing a robust solution for dynamic network analysis.

Keywords: community detection, dynamic network, higher-order structure, temporal stability

1 Introduction

Community detection (CD) has been widely applied to study the information and disease transmission, compression of network data, predictions of future individual interactions and activities, the unfolding of human mobility and so on [1, 2, 3]. Most community detection algorithms, such as stochastic block model (SBM), spectral clustering, and Louvain algorithm, are designed for static networks [4, 5, 6]. However, real-world networks are rarely static and tend to change over time. Hence, as datasets with temporal information become available, constructing dynamic networks has emerged as a new reality [7, 8, 9, 10]. A network snapshot, which aggregates all temporal edges during a time window into a static graph, is commonly used to characterize temporal networks. For instance, Figure 1(a) depicts a contact sequence, and by varying the time-window sizes, different network structures and snapshot numbers can be obtained (refer to Figure 1 (b) and (c)).

A large number of dynamic community algorithms have been developed based on network snapshots [11, 12, 13, 14]. However, the instability of community detection continues to puzzle researchers [11, 12]. Most community detection algorithms are based on quality measures, i.e, modularity. Community detection results guided by optimization quality may be quite different, although the optimization quality values are the same each run. The community instability problem was initially explored by Aynaud and Guillaume [11], who pointed out that even slight variations between consecutive network snapshots could lead to substantially different community results. They utilized multiple evaluation metrics to jointly determine dynamic communities. However, they cannot provide a universal framework for community stability. As a result, some algorithms explicitly introduce a smoothing parameter to regulate the stability of partition results for consecutive snapshots [15, 16]. This also raises novel inquiries regarding the selection of an appropriate smoothing factor. Moreover, most algorithms focus on the instability problem after the construction of network snapshots and ignore the impact of constructing network snapshots. For instance, comparing the network structure aggregated by the time window of size 6 in Figure 1(b) and the time window of size 2 in Figure 1(c), we observe the transition of the closed triangle motif $\mathcal{T}\{abc\}$ to the open triangle motifs in snapshot 2 and snapshot 3. Constructing network snapshots solely based on pairwise relationships will disregard higher-order structures, compromising the intrinsic temporal correlation between snapshots. As a result, the higher-order correlation within nodes between consecutive network snapshots will be destroyed due to the absence of corresponding higher-order traits.

In fact, a growing body of researches have proven that higher-order structures play a fundamental role in community detection [17, 18, 19]. For instance, algorithms based on triangle motifs can further enhance community detection performance [20, 21, 22]. Therefore, to comprehensively extract community structures in dynamic networks, recovering the missing higher-order structural information becomes essential. In this work, we give a novel perspective on the construction of network snapshots by making up the missing higher-order information to improve the stability of communities.

To mitigate the stability of dynamic partition, we propose a novel dynamic community detection algorithm, entitled the HOEE algorithm, which recovers the loss of higher-order information between consecutive snapshots and strengthens temporal correlations to improve the stability of dynamic communities. The HOEE algorithm effectively integrates temporal and structural higher-order information. Specifically, we define a higher-order activity potential (HAP) of nodes to quantify their activity in consecutive snapshots. Both the higher-order information of the previous network snapshot and the HAP of nodes are exploited to determine whether a current open triangle motif should be converted to a closed triangle motif, aiming to repair incomplete structures and generate corresponding enhanced networks. Finally, we utilize the Louvain algorithm to independently partition each enhanced network and identify dynamic communities. To summarize, our work contributes to the following:

1. We introduce the higher-order loss ratio (HOLR) based on the triangle motif and analyze its relationship with the stability of dynamic partitions. Experimental results demonstrate a positive cor-

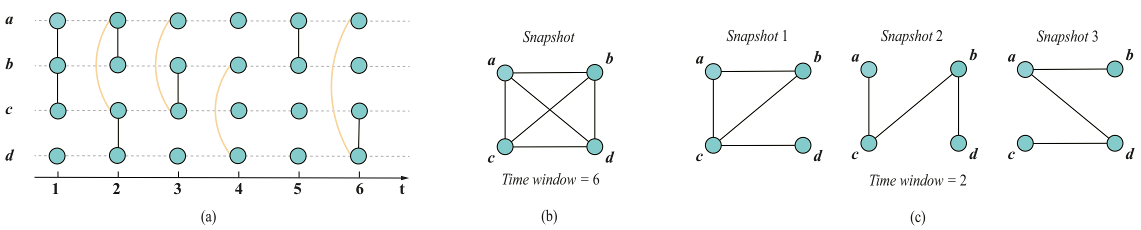

Figure 1. An illustration of a contact sequence and the process of building network snapshots with different time windows. (a) A contact sequence. (b) Network snapshot with time window of size 6. (c) Network snapshots with time window of size 2.

relation between higher-order structures and the instability of partitions.

2. We develop the HOEE algorithm, which enhances higher-order structures to detect community structures in dynamic networks.

3. A comprehensive comparison among the HOEE algorithm and the other state-of-the-art methods have been conducted on two categories of networks: synthetic and real-world dynamic networks. We present the theoretical analysis to explain the reason why the HOEE algorithm produces more consistent partitions. Additionally, we investigate the effect of the HOEE algorithm.

The rest of the paper is organized as follows. Related works are introduced in the section 2. Section 3 introduces symbols, datasets, relevant evaluation metrics, and the HOEE algorithm. Section 4 presents the experimental results. Section 5 discusses the influence of the HOEE algorithm on the graph properties. Section 6 concludes this paper.

2 Related works

2.1 Dynamic Community Algorithm

A large number of dynamic community detection algorithms based on network snapshots have been proposed [23, 24, 25, 26]. Rossetti and Cazabet [27] comprehensively surveyed these algorithms and categorized them into instant optimal CD, temporal trade-off CD and cross-time CD. Then, the incremental CD based on updated rules was introduced in [28, 29]. However, some algorithms lie outside these categories [30, 31]. These algorithms not only rely on incremental update rules but also on historical information, which we call time-dependent algorithms. Therefore, we classify dynamic community detection algorithms into instant optimal CD, temporal trade-off CD, temporal dependency CD and cross-time CD. As the concept of cross-time CD is beyond the scope of this work, we will limit our discussion to instant optimal CD, temporal trade-off CD, and temporal dependency CD.

1. Instant Optimal CD: This kind of algorithms treats community detection and evolution as two separate steps [32, 33, 34]. The key idea is to independently discover the community structure for each network snapshot, and use the similarity measure to match the community structure among different network snapshots. To achieve this, various static algorithms have been applied to each snapshot to obtain the optimal partition. Green *et al*. [25] proposed a general model for community tracking in dynamic networks by solving a classical cluster matching problem for independently detected communities on consecutive network snapshots. However, the algorithm will disrupt the temporal evolution of dynamic communities and result in instability.

2. Temporal trade-off CD: It combines community discovery and tracking simultaneously by considering the community structure of current and previous snapshots. The primary objective of these algorithms is to determine the most favorable community structure at present, while maintaining similarity between the current community structure and the previous one. All such algorithms optimize a loss function in the following form [35]:

$$Loss = \tau \cdot SL + (1-\tau) \cdot TL, \tag{1}$$

where the snapshot loss (SL) represents the loss attributed to community quality in the current snapshot, and the temporal loss (TL) corresponds to the loss caused by changes in community results between consecutive snapshots. The balance factor τ is involved to ensure balance between the two losses. To evaluate these losses precisely, certain researchers have quantified TL using normalized mutual information (NMI) and SL using modularity. To tackle the aforementioned losses, a multi-objective approach called the dynamic multi-objective genetic algorithm (DYNMOGA) was developed [36]. It formulated the detection of community structure with temporal smoothness as a multi-objective optimization problem. Another effective algorithm for dynamic community detection, named ESPRA algorithm, utilized both the resource allocation (RA) index and structural disturbance (SD) to improve the performance of dynamic partitions [37]. However, these algorithms often face challenges in accurately selecting an appropriate τ to describe the network.

3. Temporal dependency CD: This type of methods typically relies on updated rules with the historical network snapshot, and the first snapshot being identified by a static algorithm. Compared to the Louvain algorithm that executes independently for each snapshot, the DynaMo algorithm is an incremental community detection algorithm that utilizes updated rules to ensure the quality of the community structure and improve operational efficiency [28]. Contrary to the utilization of modularity-based updated rules to update the community structure of each snapshot, the C-Blondel algorithm focuses on determining whether the changed nodes are destructive nodes. Then, except destructive nodes, the remaining nodes are then compressed into super nodes. Finally, the Blondel algorithm is used to discover the community structure for each snapshot [30].

2.2 Community Instability and Temporal Smoothing

Dynamic community detection algorithms often encounter the problem of unstable dynamic partitions. Aynaud and Guillaume pointed out that even a tiny disturbance between consecutive network snapshots might result in significant alterations in the number and smoothness of the community structure [11] . As a result, their approach used constraint initialization partition to achieve the smoothness of consecutive snapshots by the Louvain algorithm. Given that the core part of the community remains consistent over time, Rosvall and Bergstrom proposed to run the same static algorithm on the same network snapshot multiple times to identify unchanged community structures [38]. Compared to unstable communities, stable communities are easier to track. Additionally, temporal trade-off community detection algorithms exhibit superiority, because they introduced a tunable parameter to balance the optimal solution and the highest similarity between consecutive snapshots. The previous methods commonly employed smoothing techniques based on the established network structure, and overlooked the instability arising from constructing network snapshots. The intrinsic correlation of temporal data becomes obscured during the process of data aggregation, consequently distorting the authentic partition of dynamic networks as a result of these smoothing operations. Moreover, they concentrated on the relationship between pairs of nodes and did not take into account the role of higher-order structure in curtailing instability.

In this work, we focus on the impact of higher-order structures on dynamic community detection.

3 Notations

3.1 Dynamic Network

A dynamic network $\mathcal{G} = (G^{(t)}, t = 1, 2, \cdots, T)$ is a series of network snapshots that change over time, where T is the length of the sequence $\mathcal{G}$. The $G^{(t)} = (V^{(t)}, E^{(t)})$ represents network structure of snapshot t, where $V^{(t)}$ and $E^{(t)}$ are the sets of nodes and edges appearing in $G^{(t)}$, respectively. The aggregation network of the dynamic network $\mathcal{G}$ is denoted by $\mathscr{G}$. The $\mathcal{A} = \{A^{(1)}, A^{(2)}, \cdots, A^{(t)}\}$ denotes the adjacency matrix of dynamic network, where $A^{(t)} \in \{0,1\}_{N\times N}$ denotes the adjacency matrix of the t-th network snapshot. $A^{(t)}_{ij} = 1$ means that node i and node j are connected in the snapshot t, and $A^{(t)}_{ij} = 0$ otherwise. In this work, only undirected networks are discussed.

3.2 Synthetic and Real-world Dynamic Datasets

1. A synthetic network with a ground-truth community is produced according to the procedure suggested by Newman and Girvan [39]. The benchmark dynamic network is generated with T=10 time steps. There are 4 communities with 64 nodes for each network snapshot. The average degree is fixed as k = 16, which represents the average number of edges connected between a node to nodes that do not belong to the community. In the synthetic network, a noise parameter z is introduced. As z increases, the community structure becomes increasingly fuzzier and more difficult to detect. In this work, we conducted experiments on this dataset with three noise levels, that is z = 2, 3 and 4, named Syn_z2, Syn_z3 and Syn_z4, respectively.

2. $Email-Eu$ was collected from email messages exchanged by members of a European research institute. Edge (u, v, t) symbolizes the mail sent by member u to member v at time t [40].

3. *Primary school* recorded face-to-face interactions among 232 students and 10 teachers of a primary school in France. Each temporal edge between two nodes corresponds to a face-to-face interaction between the two corresponding individuals. The interaction is detected by wearable sensors when the distance is less than 1.5 meters [41].

4. *Chess* is a temporal network which recorded chess players playing games with each other from 1998 to 2006. Each edge represents a game played between two chess players in time t [42].

Table 1 provides a summary of the statistics for the dynamic networks. The $|V|$ and $\mathbf{E}[|\Delta V|]$ denote the number of nodes and the average number of nodes, respectively. The $|E|$ and $\mathbf{E}[|\Delta E|]$ are the number of edges and the average number of edges in all network snapshots. # of snapshots and # triangles are the number of network snapshots and the average number of the closed triangle motifs in all network snapshots. It is important to note that the end of each time window coincides with the beginning of the next, while the duration of each window is constant. Moreover, the synthetic network has an associated ground truth, while the real-world networks do not have.

3.3 Evaluation Metrics

We employ three metrics to assess the effectiveness of dynamic community detection algorithms: temporal smoothing normalized mutual information (TS-NMI), modularity and adjusted rand index (ARI). $TS-NMI$ measures the similarity between the community structures obtained from consecutive network snapshots. Modularity assesses community quality without relying on ground-truth information. ARI is designed to measure the similarity between the community structure obtained from experimental results and that of the ground-truth.

Let C_t denotes the community structure in time step t. The NMI is defined as [43]

$$NMI\left(C_{t-1}, C_t\right) = \frac{2I\left(C_{t-1}, C_t\right)}{\left[H\left(C_{t-1}\right) + H\left(C_t\right)\right]}, \quad (2)$$

where $H(C_t)$ is the entropy of C_t, and $I(C_{t-1}, C_t)$ is the mutual information between C_{t-1} and C_t . NMI ranges from 0 to 1, where it closing to 1 indicates C_{t-1} is similar to C_t. We extend this metric to define the $TS-NMI$ value to describe the smoothness of community evolution.

$$TS-NMI = \frac{1}{T-1}\sum\nolimits_{1}^{T-1} NMI(consensus(C_{t-1}, C_t)), \quad (3)$$

where $consensus(\cdot)$ represents nodes existed in the consecutive snapshots. As $TS-NMI$ approaches 1, the community partitions between consecutive time snapshots become increasingly consistent over the set of nodes present in both snapshots, indicating a more stable and smoother community evolution

$Modularity$ [44] is a commonly employed measure of the quality of a given community structure. Given a network G and its corresponding community set C, the modularity Q is

$$Q = \frac{1}{2m}\sum\nolimits_{c\in C}\left(\alpha_c - \frac{\beta_c^2}{2m}\right), \quad (4)$$

where $\alpha_c = \sum_{i,j\in c} A_{ij}$ and $\beta_c = \sum_{i\in c} k_i$, where k_i is the degree of node i.

Let a be the number of pairwise nodes in the same community in both experiment results C_e and

Table 1. Description of synthetic and real-world dynamic networks

Datasets	$\lvert V\rvert$	$\mathbf{E}[\lvert\Delta V\rvert]$	$\lvert E\rvert$	$\mathbf{E}[\lvert\Delta E\rvert]$	# of snapshots	# triangles
Syn_z2	256	256	4096	4096	10	1163
Syn_z3	256	256	4096	4096	10	827
Syn_z4	256	256	4096	4096	10	711
Email-Eu	986	707	332334	3511	18	4904
Primary school	242	186	8317	682	26	901
Chess	7301	1504	62385	3700	17	1662

ground truth community C_g, b be the number of pairwise nodes in the same community in C_e and in different communities in C_g, c be the number of pairwise nodes in different communities in C_e and in the same community in C_g, d be the number of pairwise nodes in different communities in both C_e and C_g. ARI is defined as

$$ARI(C_e,C_g) = \frac{2(ad-bc)}{b^2+c^2+2ad+(a+d)(b+c)}, \tag{5}$$

where its upper bound is 1. The higher ARI is, the better the detected communities are [45].

It is noteworthy that $TS-NMI$ and ARI are appropriate measures only for networks that have a ground-truth available, whereas Q can be calculated irrespective of ground-truth information. A larger value of $TS-NMI$, Q and ARI implies superior performance of the method.

3.4 HOEE Algorithm

For different dynamic networks, the most used modeling method is to build network snapshots. Building network snapshots based on the node pairwise alone does not cause the information loss from the perspective of the lower-order dynamic model. In fact, when we put the perspective on a higher-order level, the loss of higher-order information is unavoidable. It's worth to explore the impact of higher-order loss on the community detection results. We first introduce the higher-order structure, i.e., the network motif. Then, we explore the relationship between the missing higher-order information and stability. Finally, we introduce the HOEE algorithm.

Network motif is a typical higher-order structure and the community detection algorithm based on motif has been proposed in [46, 47, 48].

Definition 1. *Network motif is the interconnection pattern that occurs in a real-world network, and the number of interconnection patterns in real-work networks appears significantly higher than that in a corresponding random network [49]. The network motif M_n^p can be expressed as*

$$M_n^p = (\upsilon_M, \varepsilon_M), \tag{6}$$

where $\nu_M \in V$ is the set of n nodes that appear in the motif, and $\varepsilon_M \in E$ is the set of p edges that appear in the motif. Specifically, M_n^p is a network subgraph consisting of n nodes and p edges. That is, the subgraph can range from the spanning tree structure with $p = n-1$ to the clique structure (i.e. $p = n(n-1)/2$). We use M_n^p to represent a specific motif with n nodes and p edges, for instance, M_3^3 indicates a motif with 3 nodes and 3 edges.

Definition 2. *Motif instance, denoted by $I(M_n^p)$, is a specific appearance of motif in the network.*

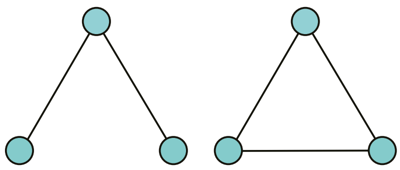

(a) M_3^2. (b) M_3^3.

Figure 2. Schematic of the fundamental 3-node network motifs. (a) The open triangle motif (denoted as M_3^2), consisting of 3 nodes and 2 edges. (b) The closed triangle motif (denoted as M_3^3), comprising 3 nodes and 3 edges.

A network motif M_n^p include the $\mathbf{s}$ motif instances, i.e, motif instance set $\{I_1(M_n^p), I_2(M_n^p), \cdots, I_{\mathbf{s}}(M_n^p)\}$.

Since triangle structures play an important role in community detection, we focus on the triangle motif in the work. We explore the motif instance M_3^3, on the basis of which the higher-order loss ratio

($HOLR$), that is, the missing higher-order structure caused by modeling network evolution as network snapshots. The relationship between the $HOLR$ and $TS-NMI$ will be studied with attention.

Definition 3. *Higher-order loss ratio (HOLR). The HOLR represents the ratio of the num of higher-order structures in different networks.*

$$HOLR = \frac{|\{M \in \mathcal{G}_{new}\}|}{|\{M \in \mathcal{G}\}|}, \tag{7}$$

where M represents the specific motif instance M_3^3 in graphs $\mathcal{G}_{new}$ and $\mathcal{G}$, respectively. $\{\cdot\}$ represents the set of $\cdot$ and $|\cdot|$ represents the number of $\cdot$. In this work, $\mathcal{G}_{new}$ represents the new network generated from the aggregated network by removing nodes.

The $HOLR$ characterizes the loss of higher-order structure caused by modeling network evolution as network snapshots. The $TS-NMI$ represents the stable community results. In order to explore the relationship between the higher-order loss and stability of community detection in dynamic networks, we study how the $TS-NMI$ changes with $HOLR$. We perform the following steps:

(i) Construct the dynamic network into an aggregated network and order the nodes in degrees in the aggregated network.

(ii) Starting from the small-degree nodes, we remove the percentage of the total number of nodes sequentially and reconstruct a new network $\mathcal{G}_{new}$ with the remaining edges.

(iii) The Louvain algorithm is used to detect the community structure of each new network $\mathcal{G}_{new}$.

(iv) We calculate the $HOLR$ and the corresponding $TS-NMI$ between the new network $\mathcal{G}_{new}$ and the aggregated network $\mathcal{G}$.

To mitigate the influence by randomness in the Louvain algorithm, we conduct the experiments for 100 times to obtain the average results as the final $TS-NMI$.

Figure 3 demonstrates that the $TS-NMI$ decreases with the increase of $HOLR$ in all six temporal networks. Therefore, reducing the value of $HOLR$ is necessary to improve temporal smoothness. One of the sources of $HOLR$ is due to model the network snapshots in a temporal network. To address this issue, we propose the HOEE algorithm that recovers missing higher-order structures to enhance temporal stability by reconnecting effective edges.

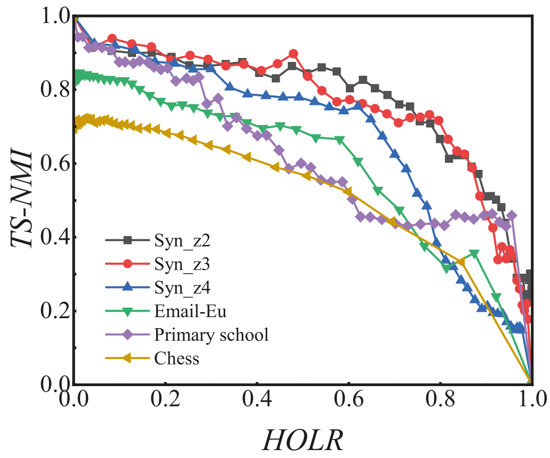

Figure 3. $TS-NMI$ at different $HOLR$ in the synthetic and real-word temporal networks.

Figure 4 exhibits a practical instance of dynamic edge enhancement from an open triangle motif to closed triangle motif from time $t-1$ to time t. The aim is to investigate the necessity of this process of edge enhancement between consecutive snapshots. To enhance higher-order edges, two aspects are to be concentrated on: first, whether the higher-order structure and the new connected edge previously existed, and second, the propensity of the two nodes to link with each other.

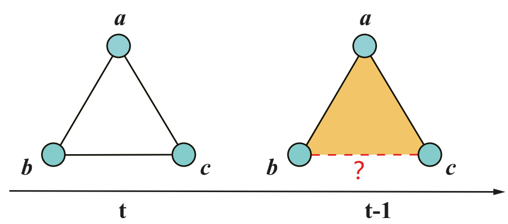

Figure 4. Illustrative example of edge enhancement between an open triangle motif and a closed triangle motif under consecutive snapshots. The formation of link e_{bc} make an open triangle motif $O\{abc\}$ at snapshot $t-1$ become a closed triangle motif $\mathcal{T}\{abc\}$ at snapshot t.

One of the reasons of disappearing closed motifs is due to the high temporal resolution when building the network snapshots. Therefore, we first posit that only closed triangle motifs from the previous network snapshot aid in the conversion of an open triangle motif into a closed triangle motif in the current network snapshot. This also means that the added edges must appear in the previous network snapshot. It seems illogical to reconnect nonexistent edges from the prior snapshot, as discussing nonexistent routes between two airports in the US air transport network is illogical. Second, we aim to deduce the propensity of pairwise nodes to strengthen their connections across successive snapshots, which reflects the level of active connections between the node and other nodes. To accomplish this, we need to introduce novel concepts. In light of this, we propose the higher-order activity potential (*HAP*) of each node as a measure to judge whether the new edge needs to be added between nodes.

Algorithm 1 HOEE algorithm

Require: Dynamic network $\mathcal{G} = \{G^{(1)}, G^{(2)}, \cdots, G^{(t)}\}$, β_1, β_2
Ensure: $\{C^{(1)}, C^{(2)}, \cdots, C^{(t)}\}$

$C^{(1)} \leftarrow Louvain(G^{(1)})$
for $t = 2 : T$ **do**
  Construct harmonic motif adjacency matrix HMA from $A^{(t)}$ via Equation (10).
  Construct participation adjacency matrix PM from $HMA(t)$ via Equation (9).
  Compute HAP_i of every node i via Equation (8).
  $\Delta E \leftarrow$ a set of edges changed from $E^{(t-1)}$ to $E^{(t)}$.
  for $e_{ij} \in \Delta E$ **do**
    randomly generate a threshold: $thres$.
    if $thres <= \beta_1$ **then**
      if $HAP_i < \beta_2$ and $HAP_j < \beta_2$ **then**
        continue
      end if
    end if
    active_edge.append(e_{ij})
  end for
  for $e_{ij} \in active\_edge$ **do**
    hybrid_G = $G^{(t)}$ + active_edge
    tri = $detect\_tri$(hybrid_G)
    if i in tri and j in tri **then**
      $enhance\_G^{(t)}.add\_edge(e_{ij})$
    end if
  end for
  $C^{(t)} \leftarrow Louvain(G^{(t)})$
end for

The HAP_i indicates the activity of node i in the consecutive network snapshots, which is defined as

$$HAP_i = \frac{1}{2} \frac{\sum_j p_{ij}(t)\, p_{ij}(t+1)}{\sqrt{\left[\sum_j p_{ij}(t)\right]\left[\left[\sum_j p_{ij}(t+1)\right]\right]}}, \tag{8}$$

where p_{ij} signifies the extent of edge e_{ij} involved in the higher-order structure. It additionally measures the proximity between node i and node j at time t. The specific definition of the participation matrix (PM, $PM = \{p_{ij}\}_{N*N}$) is provided in definition 4.

Definition 4. *PM: the ratio of the higher-order structure e_{ij} participated in the network. The p_{ij} of edge e_{ij} at snapshot t is defined as*

$$p_{ij}(t) = \frac{w_{ij}(t)}{\sum_{k \in N_t(i)} w_{ik}(t) + \sum_{k \in N_t(j)} w_{jk}(t)}, \tag{9}$$

where $N_t(i)$ represents the neighbor of node i at network snapshot t, and $w_{ij}(t)$ represents the harmonic proportion of the number of open and closed triangle motifs that involve the edge e_{ij} at snapshot t. We define the harmonic motif adjacency matrix at snapshot t, denoted $HMA(t)$, $HMA(t) = \{w_{ij}\}_{N*N}$.

Definition 5. *Harmonic Motif Adjacency matrix (HMA): the harmonic adjacency matrix of motif instances is defined as the weight assignment between motif instances M_3^2 and M_3^3. The w_{ij} of edge e_{ij} at snapshot t is defined as*

$$w_{ij}(t) = \lambda M_3^3 + M_3^2, \tag{10}$$

where λ is a harmonic parameter, which distinguishes the effects of different motif instances. When selecting the parameter λ, we posit that a closed triangle motif can be constructed from three open triangle motifs. This implies that the weight of a closed triangle motif is three times that of an open triangle motif.

The details of the HOEE algorithm are presented in Algorithm 1. The input contains the dynamic network $\mathcal{G}$ and parameters β_1 and β_2, which range from 0 to 1. The output contains the final dynamic communities. Algorithm 1 also can be described as follows:

(i) We construct the harmonic motif adjacency matrix and calculate the participation matrix according to Equation (9). From the participation matrix, we obtain the HAP of each node in the current snapshot using Equation (8).

(ii) To assess the activation status of changed edges between two consecutive snapshots, it is necessary to determine whether the edge is active. β_2 is used to evaluate whether two nodes exhibit a tendency to strengthen their connection across these snapshots. In line 9, β_1 is employed to ascertain the necessity of higher-order reinforcement.

(iii) The triangle motifs are found in the original network by the process of $detect\_tri$ which is proposed by Ahmed *et al* [50].

(iv) The original network is enhanced.

(v) Perform the Louvain algorithm for each enhanced network to detect the community structure. The dynamic community structures with temporal stability are extracted.

The algorithm framework is shown in Figure 5. It is noteworthy that for the first snapshot, the community structure is implemented by the Louvain algorithm in the original network. Moreover, the Louvain algorithm is employed to identify community structures in the enhanced network, without fundamentally altering the original network. Additionally, as high-degree nodes are not always stable [51], we will randomly eliminate some new added edges.

4 Results

In this section, we compare the HOEE algorithm to six advanced algorithms: Louvain (static), Infomap (static), ESPRA, C_Blondel, DynaMo, and ComSP. These algorithms represent different types of dynamic community detection methods described in the pre-mentioned section. Table 2 presents the experimental results obtained from synthetic and real-world dynamic networks. For reliable results, each experiment is conducted 100 times and the averages are recorded.

Infomap: It's one of the most popular community detection algorithms, which optimized the objective function known as the map equation.

ESPRA: ESPRA is a community detection method based on network structural perturbation and topological similarity for dynamic networks.

C_Blondel: The algorithm aims to find destructive nodes between consecutive snapshots, and compresses the remaining nodes as super nodes except the destructive nodes as the compressed graph. The Blondel algorithm is used to find the community structure for the compressed graph.

DynaMo: A new modularity-based dynamic community detection algorithm, which can effectively identify communities of dynamic networks than using static algorithms.

ComSP: The algorithm leverages the encoding–decoding scheme present in a succinct network representation method to reconstruct each snapshot via a common low-dimensional subspace to detect dynamic community structure [26].

Table 2 summarizes the average performance of various algorithms on all network snapshots, with the highest values in bold. The proposed algorithm outperforms other algorithms in all evaluation metrics for the three synthetic datasets, particularly in regard to $TS-NMI$ and ARI. Additionally, the HOEE algorithm maintains stable dynamic partitions without compromising the quality of community partitions for each snapshot. As z-value increased, the community structures became more ambiguous, resulting in significant differences in $TS-NMI$. The HOEE algorithm and the Louvain-based algorithms consistently performed better than non-Louvain algorithms for Syn_z2, which has a clear and easy-to-detect network structure. Conversely, for Syn_z3 and Syn_z4, with complex and difficult-to-detect network structures, the compared algorithms failed to maintain dynamic community stability and accurately identify dynamic community structures, while our algorithm maintained high accuracy and stability. In scenarios where the network structure becomes blurred, the significance of time-sensitive higher-order information increases for community detection. The HOEE algorithm exhibits superior effectiveness and robustness compared to the three datasets.

Figure 6 depicts $TS-NMI$, ARI, and modularity results of our algorithm and the compared algorithms for each network snapshot. The figure clearly shows that our algorithm outperforms the compared algorithms for most of the snapshots. The results of the synthetic dataset demonstrate that the HOEE algorithm can not only accurately track community evolution and maintain quality, but also

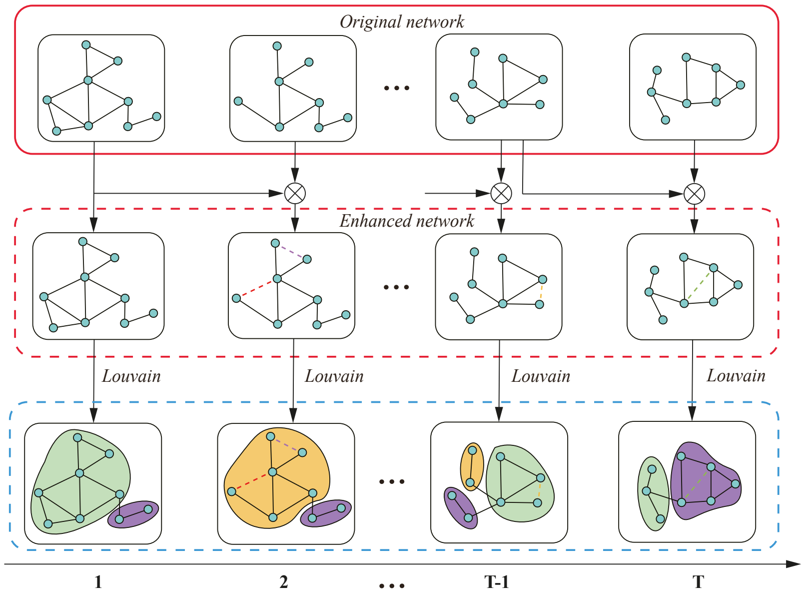

Figure 5. Illustration of the HOEE algorithm framework. The original network is contained within the solid red box, while the enhanced network is within the dotted red box. The multiplier denotes the enhanced network derived from the corresponding original network.

Table 2. Performance comparison of the proposed method and advanced methods in the synthetic and real-world network. The top performance is highlighted in bold.

Datasets	metrics	Louvain	Infomap	ESPRA	DynaMo	C_Blondel	ComSP	HOEE
Syn_z2	TS-NMI	**0.7**	0.30	0.44	**0.7**	**0.7**	0.57	**0.7**
	modularity	**0.49**	0.27	0.4	**0.49**	**0.49**	0.01	**0.49**
	ARI	**1.00**	0.48	0.68	**1.00**	**1.00**	0.04	**1.00**
Syn_z3	TS-NMI	0.59	0.15	0.34	0.61	0.58	0.02	**0.66**
	modularity	**0.36**	0.05	0.28	**0.36**	**0.36**	0.00	**0.36**
	ARI	0.92	0.02	0.57	0.92	0.92	0.00	**0.95**
Syn_z4	TS-NMI	0.10	0.14	0.06	0.27	0.10	0.01	**0.45**
	modularity	**0.23**	0.03	0.16	**0.23**	**0.23**	0.00	**0.23**
	ARI	0.22	0.01	0.23	0.54	0.22	0.01	**0.67**
Email-Eu	TS-NMI	0.76	0.68	0.30	0.51	0.76	0.80	**0.82**
	modularity	**0.49**	0.45	0.00	**0.49**	0.37	0.47	**0.49**
Primary school	TS-NMI	0.85	0.75	0.63	0.80	0.79	0.77	**0.90**
	modularity	**0.74**	0.68	0.24	0.72	**0.74**	**0.74**	**0.74**
Chess	TS-NMI	0.36	0.22	0.25	0.29	0.20	0.20	**0.37**
	modularity	**0.74**	0.54	0.01	0.62	0.72	**0.74**	**0.74**

achieve the smoothness of dynamic partitions. Interestingly, we observe that the temporal stability of other baseline algorithms begins to decline while the HOEE algorithm continues to perform very well.

The HOEE algorithm also performs well on real-world datasets, especially when evaluated using $TS-NMI$. Specifically, $TS-NMI$ of our algorithm rank highest compared to other methods. Additionally, the HOEE algorithm significantly improves the stability of communities while maintaining the quality of detected communities. A comparison of the performance of the proposed algorithm and other algorithms is presented in Figure 7, where the evolution of $TS-NMI$ and modularity for each

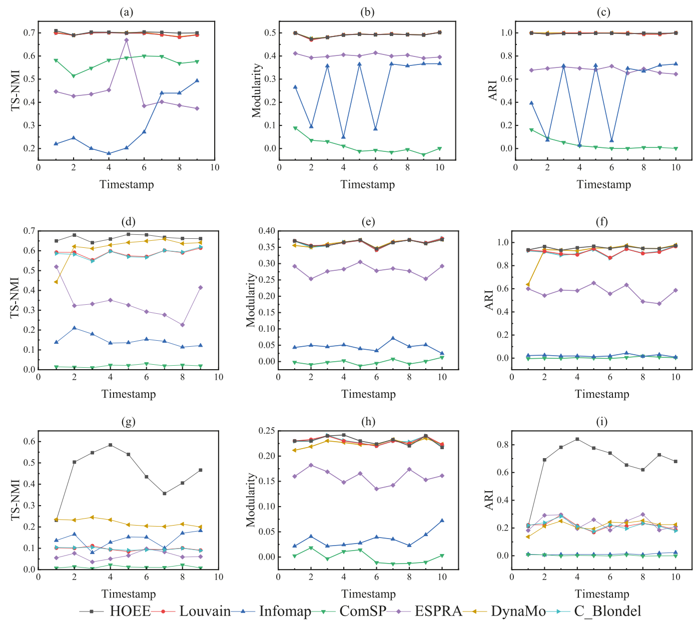

Figure 6. The $TS-NMI$, *modularity* and ARI values of the synthetic network.(a),(b) and (c) Syn_z2. (d),(e) and (f) Syn_z3. (g),(h) and (i) Syn_z4.

network snapshot is demonstrated. Although it may not achieve the highest score in every snapshot, the HOEE algorithm consistently ranks in the top two for both $TS-NMI$ and modularity, always outperforming Louvain-based algorithms.

Here, we investigate the extent to which community detection algorithms accurately reproduce the number of communities. We compare the number of dynamic communities detected by the aforementioned algorithms in a synthetic network with the actual number of communities, as depicted in Figure 8. The box plot is employed to visualize the number of communities detected by each algorithm for the three synthetic datasets. The average value is indicated by a gray solid line in the center of each box. To provide clarity, Figure 8(a) and Figure 8(b) depict the average numbers across all snapshots of the algorithms applied to the datasets Syn_z2 and Syn_z3, respectively. It can be seen that with the exception of Infomap and ESPRA, other algorithms can accurately discover the true number of communities in most cases. For each snapshot, separate box plots are presented in Figure 8(c)-(h), demonstrating the number of communities detected by each algorithm for the dataset Syn_z4. We find that when the network is blurred, the comparison algorithm can no longer accurately find the number of communities, and our algorithm can still accurately approach the number of communities in most cases. This indicates that the proposed algorithm possesses a notable advantage in community detection by inferring the number of communities. Therefore, our algorithm has the potential to provide superior initializations for some methods that require prior knowledge of the number of communities [16, 52, 53].

To summary, the proposed HOEE algorithm works well on these dynamic network especially when $TS-NMI$ is adopted as the evaluation measure. We prioritize the $TS-NMI$ measure because it reflects the stability of the community structure in each snapshot. Additionally, we discovery that the HOEE algorithm improves the overall quality of communities. Although it cannot consistently outperform other methods in every snapshot, the HOEE algorithm achieves the highest average rankings. Moreover, the HOEE algorithm also allows us to better identify the true community number.

5 Discussions

In this section, we present a theoretical analysis of the HOEE algorithm in terms of stability maintenance. Additionally, we investigate the impact of the proposed algorithm on the graph structure, which provides novel insights into dynamic

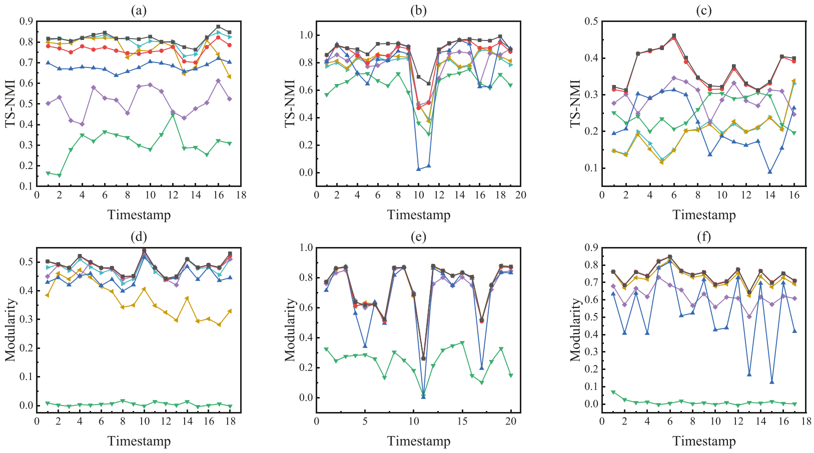

Figure 7. The $TS-NMI$ and modularity results of the real-world networks.(a) and (d) Email-Eu. (b) and (e) Primary school. (c) and (f) Chess.

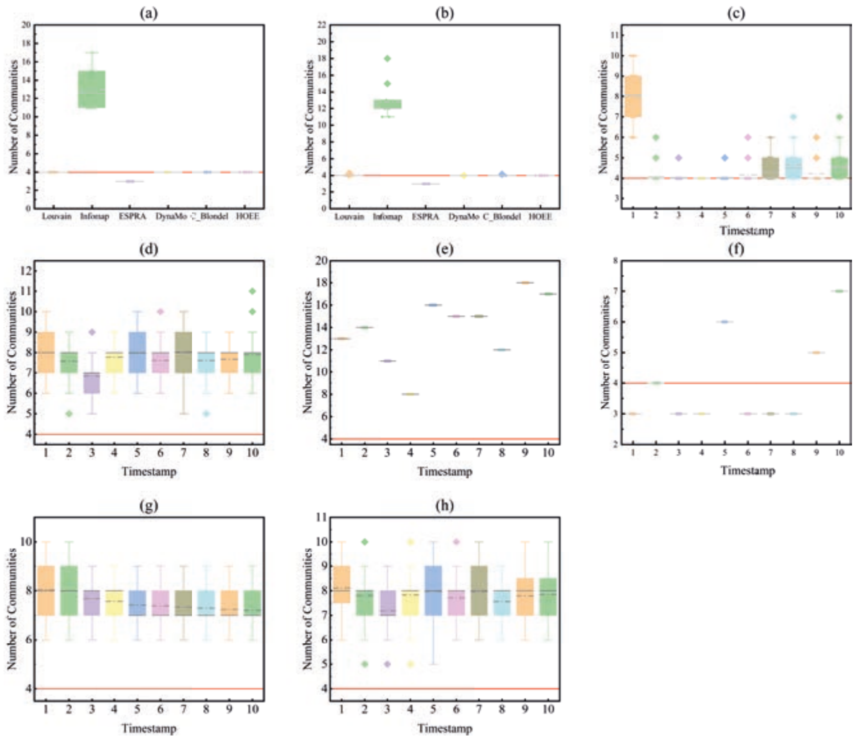

Figure 8. Number of dynamic communities on synthetic networks: Syn_z2 (subplot (a)), Syn_z3 (subplot (b)) and Syn_z4 (subplots (c)–(h)). Each point corresponds to the community number detected by six methods in subplot (a) and subplot(b). For the dataset Syn_z4, subplot(c)-(h) shows the number of community partitions on each network snapshot by six methods, i.e. HOEE, Louvain, Infomap, ESPRA, DynaMo and C_Blondel, respectively.

networks. Furthermore, we examine the influence of parameters on the performance of the proposed algorithm.

5.1 Stability Analysis of HOEE Algorithm

In the HOEE algorithm, the Louvain method is employed to partition the enhanced network, with the aim of optimizing the modularity. When new edges are added, this will affect the aggregation tendency between nodes. Consider the scenario where the clique (i, j, u) belonged to the same community C_1 in the snapshot t. In the snapshot $t+1$, these nodes form an open triangle motif, where nodes j and u are not connected.

Proof: when the new edge between node j and node u is connected, it will make node j more inclined to join the same community where node i and node j belong to.

$$Q^{t+1} = \frac{1}{M+m}\left(\left[l_{c_p}+a-\frac{(d_{c_p}+2x)^2}{4(M+m)^2}\right]+\left[l_{c_q}-\frac{(d_{c_q}+y)^2}{4(M+m)^2}\right]\right),$$
$$Q^t = \frac{1}{M+m}\left(\left[l_{c_p}-\frac{(d_{c_p}+x)^2}{4(M+m)^2}\right]\left[l_{c_p}+y-\frac{(d_{c_p}+2y)^2}{4(M+m)^2}\right]\right),$$

$$Q^{t+1}-Q^t = \frac{1}{4(M+m)^2}\left(2a(2M-d_{c_p})-2b(2M-d_{c_q})\right.$$
$$\left.+x(4m-3x)-y(4m-3y))\right). \tag{11}$$

When $x=1$ and $y=0$, $2M-d_{c_p}\geq 0$, $m-x\geq 0$, that is $Q^{t+1}-Q^t\geq 0$. Hence, the conclusion follows.

5.2 Impact of New Edges on Graph Properties

We explore the impact of newly added edges on graph properties.

5.2.1 Node Degree Correlation Analysis

We posit that nodes with a high degree, i.e. degree exceeding the average degree of the graph, would be classified as high-degree nodes. Conversely, nodes with the degree lesser than the average degree would be tagged low-degree nodes. Subsequently, we investigate three cases: L-L, S-S, and L-S. L-L characterizes scenarios where high-degree nodes are linked, S-S represents situations where low-degree nodes connect, and L-S pertains to occurrences whereby high-degree nodes are connected with low-degree nodes. Of the three cases, L-L has the highest proportion in all snapshots depicted in Figure 9. This indicates that the HOEE algorithm constructs enhanced networks with significant degree correlations, despite its focus on higher-order structures. The prevalence of stable L-L connections aligns with the tendency toward homophily in real-world networks (e.g., preferential attachment among central nodes) and contributes to enhanced temporal stability.

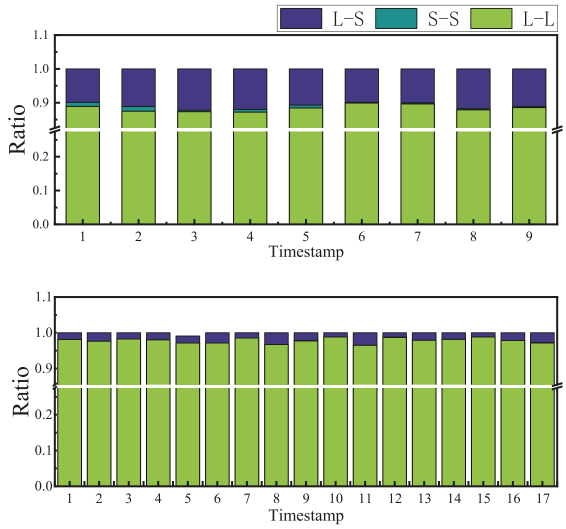

Figure 9. Degree distribution of newly added edges.

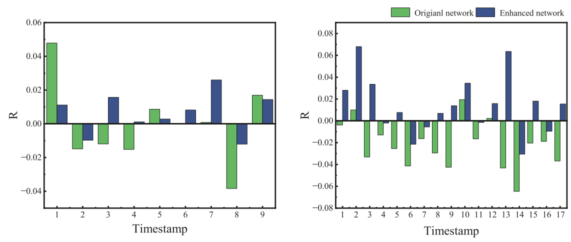

Figure 10. Comparison of the assortativity coefficients of the original network (green) and the corresponding enhanced network (blue), where the right picture is Syn_z2 and the left picture is Email-Eu.

5.2.2 Assortativity Shifts

Assortativity, initially proposed by Newman, is quantified by the Pearson correlation coefficient of degree-degree pairs [54]. We evaluate the assortativity coefficients R of both the original and enhanced networks, which are presented in Figure 10. Our analysis reveals that the assortativity R of the original network can vary substantially from that of the enhanced network. Furthermore, most of the network snapshots demonstrate a trend towards homogeneity. It is noteworthy that, in situations where the initial network is disassortative, R always increases in the enhanced networks. However, the situation becomes complex when the original networks are assortative. Although most of the enhanced networks have larger R, some may showcase smaller R. We contend that this outcome is contingent on the existing network structure. If high-degree nodes are already well-connected, establishing additional edges may instead introduce heterogeneity.

5.2.3 Higher-Order Clustering Effects

We further examine the influence of the HOEE algorithm on the higher-order clustering coefficient, a crucial network property defined as the probability of clique closure, conceptualized through clique expansion [55]. For a node u in the network, its ζ-order clustering coefficient is

$$c_\zeta(u) = \frac{\zeta\left|Z_{\zeta+1}(u)\right|}{W_\zeta(u)}, \tag{12}$$

where $Z_{\zeta+1}(u)$ represents the collection of (ζ+1)-clique containing node u, and $W_\zeta(u)$ implies the set of ζ-order wedge structures centered on node u. To obtain a non-zero ζ-order cluster coefficient, the central node of a ζ-order wedge structure must have one. The local ζ-order clustering coefficient of the network equals the average of the ζ-order cluster coefficients of all such nodes, i.e.:

$$\overline{C_\zeta} = \frac{1}{\widetilde{V_\zeta}} \sum\nolimits_{u\in\widetilde{V_\zeta}} C_\zeta(u), \tag{13}$$

where $\widetilde{V_\zeta}$ denotes the group of nodes positioned centrally in a minimum of one ζ-order wedge structure. We calculate the second-order cluster coefficient $\overline{C_2}$ and the third-order clustering coefficient $\overline{C_3}$ of the network.

Nodes connected by a new edge are designated as affected nodes. We rank these nodes by their number of new connections and analyze the top 20%. As shown in Table 3, the average higher-order clustering coefficient for these top affected nodes increases significantly in the enhanced network compared to the original. This observation suggests that the HOEE algorithm strengthens the cohesiveness among central nodes, and that enhancing this local compactness aids in maintaining temporal stability.

In summary, networks enhanced by the HOEE algorithm demonstrate a tendency towards increased assortativity, particularly when the original network exhibits disassortative mixing. Furthermore, heightened local compactness among nodes promotes greater temporal smoothness in dynamic community evolution. Although the introduction of new edges generates both open and closed triangle motifs, the predominance of closed triangles enhances the structural stability of dynamic communities. Therefore, to improve the stability of a dynamic community, strategically enhancing connections among high-degree nodes is most conducive to achieving smoother temporal transitions.

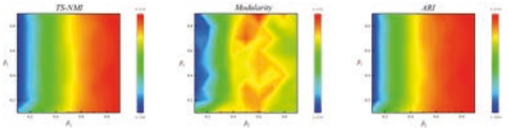

Figure 11. Performance of our method on the synthetic datasets Syn_z4. The heat maps in this figure show the results $TS-NMI$, modularity and ARI under β_1 and β_2.

5.3 Parameter Sensitivity Analysis

In the proposed algorithm, two parameters, β_1 and β_2, are used to determine whether to connect two distinct nodes. We conduct an investigation to determine the effects of these parameters on the performance of the HOEE algorithm. As an example, we analyze the performance of the HOEE algorithm on the synthetic dataset Syn_z4, under varying parameter settings. In Figure 11, we demonstrate that altering β_1 and β_2 leads to minimal change in the results, while the overall quality of the HOEE algorithm remains unaltered. Hence, the HOEE algorithm is capable of withstanding changes in the parameters, exhibiting robustness. Moreover, our analysis reveals that while determining β_1, an increase in β_2 leads to an increase in values of $TS-NMI$ and ARI, whilst the modularity rises initially and descends. Among the two parameters, β_2 has a more significant impact on the value of the evaluation metrics compared to β_1.

We are most concerned about the value of $TS-NMI$, and it is clear from the results that even in the worst case, the partition result in the enhanced network is still much better than the result in the original network. We also find that $TS-NMI$, modularity, and ARI have the same tendencies within different parameter values.

5.4 Time Complexity Analysis

Considering the characteristics of the HOEE algorithm, two main properties are shown: (1) It can

Table 3. Average local higher-order clustering coefficients for the top-20% of affected nodes in synthetic and real-world networks

	$\overline{C_2}$		$\overline{C_3}$	
	original network	enhanced network	original network	enhanced network
SYN_z2	0.1115	0.1964	0.0197	0.0635
SYN_z3	0.0796	0.1354	0.0087	0.0304
SYN_z4	0.0667	0.1292	0.0045	0.0197
Email-Eu	0.2225	0.2543	0.1337	0.1616
Primary school	0.3660	0.4402	0.1972	0.2760
Chess	0.2031	0.2133	0.1243	0.1254

be used incrementally on precomputed sets of communities; (2) Considering the enhancement of the edge, it depends only on two consecutive network snapshots. Therefore, the time complexity of the algorithm only needs to consider two consecutive moments.

The proposed HOEE algorithm is comprised of two phases; the first one is to calculate the active potential energy of nodes in snapshots. The main time consumption in this phase is higher-order structures. There are T network snapshots. Assuming network snapshot t would be enhanced. The number of edges in snapshot t-1 and snapshot t are $\left|E^{t-1}\right|$ and $|E^t|$, respectively. Δ^t_{max} is the maximum degree in the snapshot t. The time complexity of the snapshot t is accomplished in $O(|E^t|\Delta^t_{max})$. Then the number of new connected edges is $|\Delta E^t|$.

The second phase is used to detect the community structure using Louvain. It can be carried out with $O(|E^t|+|\Delta E^t|)$ time consumption in the enhanced network.

Therefore, the proposed method can detect communities from networks with O(T $\cdot$ $|E^t|\cdot\Delta_{max}$ + (T-1) $\cdot$ ($|E^t|$ + $|\Delta E^t|$)) time complexity.

In fact, since our algorithm only has the dependence of two consecutive network snapshots, and there is no global dependency, the use of distributed algorithms can greatly shorten the running time.

6 Conclusion

In this work, we present a novel dynamic community detection algorithm called the HOEE algorithm, which aims to recover the loss of higher-order information that results from building network snapshots. The algorithm defines HAP of nodes, then combines this pattern with historical higher-order information to determine whether open triangle motifs should be converted to closed triangles, thereby enhancing connectivity between consecutive snapshots. Community detection on each enhanced network is performed independently using the Louvain algorithm. Extensive experiments on synthetic and real-world dynamic networks evaluate the proposed method's performance. Comparisons with state-of-the-art algorithms using $TS-NMI$, ARI, and modularity metrics demonstrate that our approach alleviates instability in dynamic community partitions and extracts high-quality community structures. Furthermore, as the method relies solely on historical information, it supports online community structure tracking in dynamic networks.

References

[1] J. Zhao and K. H. Cheong, Mase: Multi-attribute source estimator for epidemic transmission in complex networks, IEEE Transactions on Systems, Man, and Cybernetics: Systems, vol. 54, no. 6, pp. 3308–3320, 2024.

[2] T. P. Peixoto, Network reconstruction via the minimum description length principle, Physical Review X, vol. 15, no. 1, p. 011065, 2025.

[3] J. Qian, W. Tong, M. Ling, X. Du, and H. Ding, Pixel-based clustering for local interpretable model-agnostic explanations, Journal of Artificial Intelligence and Soft Computing Research, vol. 15, no. 3, pp. 257–277, 2025.

[4] V. D. Blondel, J.-L. Guillaume, R. Lambiotte, and E. Lefebvre, Fast unfolding of communities in large networks, Journal of statistical mechan-

ics: theory and experiment, vol. 2008, no. 10, p. P10008, 2008.

[5] P. W. Holland, K. B. Laskey, and S. Leinhardt, Stochastic blockmodels: First steps, Social networks, vol. 5, no. 2, pp. 109–137, 1983.

[6] M. A. Kłopotek, B. Starosta, and S. T. Wierzchoń, Eigenvalue-based incremental spectral clustering, Journal of Artificial Intelligence and Soft Computing Research, vol. 14, no. 2, pp. 157–169, 2024.

[7] L. Ni, Q. Li, Y. Zhang, W. Luo, and V. S. Sheng, Lsaden: local spatial-aware community detection in evolving geo-social networks, IEEE Transactions on Knowledge and Data Engineering, vol. 36, no. 7, pp. 3265–3280, 2024.

[8] P. Jiao, X. Zhang, Z. Liu, L. Zhang, H. Wu, M. Gao, T. Li, and J. Wu, A deep contrastive framework for unsupervised temporal link prediction in dynamic networks, Information Sciences, vol. 667, p. 120499, 2024.

[9] M. Zalasiński, A. Cader, Z. Patora-Wysocka, and M. Xiao, Evaluating neural network models for predicting dynamic signature signals, Journal of Artificial Intelligence and Soft Computing Research, vol. 14, 2024.

[10] C.-C. Hsu, L. Hsu-Chao, G.-Y. Jhang, J.-L. Huang, and W. Jun-Zhe, Nest: A novel ensemble method for estimating spatio-temporal gait parameters using inertial measurement units, Journal of Artificial Intelligence and Soft Computing Research, vol. 15, no. 4, pp. 319–336, 2025.

[11] T. Aynaud and J.-L. Guillaume, Static community detection algorithms for evolving networks, in 8th International Symposium on Modeling and Optimization In Mobile, Ad Hoc, and Wireless Networks. IEEE, 2010, pp. 513–519.

[12] M. J. Bommarito II, D. M. Katz, and J. L. Zelner, On the stability of community detection algorithms on longitudinal citation data, Procedia-Social and Behavioral Sciences, vol. 4, pp. 26–37, 2010.

[13] L. Zhang, C. Qin, H. Yang, Z. Xiong, R. Cao, and F. Cheng, A diversified population migration-based multiobjective evolutionary algorithm for dynamic community detection, IEEE Transactions on Emerging Topics in Computational Intelligence, 2024.

[14] J. Zhao, L. Zhou, C. Liu, Y. Jiang, S. Kwong, and Z.-H. Zhan, Multimodule-based dynamic community detection for enhancing innovation performance in crowdsourcing contests, IEEE Transactions on Systems, Man, and Cybernetics: Systems, 2025.

[15] Y.-R. Lin, Y. Chi, S. Zhu, H. Sundaram, and B. L. Tseng, Facetnet: a framework for analyzing communities and their evolutions in dynamic networks, in Proceedings of the 17th international conference on World Wide Web, 2008, pp. 685–694.

[16] X. Zeng, W. Wang, C. Chen, and G. G. Yen, A consensus community-based particle swarm optimization for dynamic community detection, IEEE transactions on cybernetics, vol. 50, no. 6, pp. 2502–2513, 2019.

[17] S. Krishnagopal and G. Bianconi, Spectral detection of simplicial communities via hodge laplacians, Physical Review E, vol. 104, no. 6, p. 064303, 2021.

[18] X. Wu, C.-D. Wang, J.-Q. Lin, W.-D. Xi, and P. S. Yu, Motif-based contrastive learning for community detection, IEEE Transactions on Neural Networks and Learning Systems, vol. 35, no. 9, pp. 11 706–11 719, 2024.

[19] M. Chen, S. Wang, M. Leng, Y. Chen, and Y. You, Core triangle motif-driven local community detection algorithm, IEEE Transactions on Computational Social Systems, pp. 1–12, 2025.

[20] P.-Z. Li, L. Huang, C.-D. Wang, and J.-H. Lai, Edmot: An edge enhancement approach for motif-aware community detection, in Proceedings of the 25th ACM SIGKDD international conference on knowledge discovery & data mining, 2019, pp. 479–487.

[21] P.-Z. Li, L. Huang, C.-D. Wang, J.-H. Lai, and D. Huang, Community detection by motif-aware label propagation, ACM Transactions on Knowledge Discovery from Data (TKDD), vol. 14, no. 2, pp. 1–19, 2020.

[22] J. Xiao, Y.-W. Wei, J. Cao, and X.-K. Xu, Higher-order fuzzy membership in motif modularity optimization, IEEE Transactions on Fuzzy Systems, vol. 32, no. 12, pp. 7143–7156, 2024.

[23] W. Wang and X. Li, Temporal stable community in time-varying networks, IEEE Transactions on Network Science and Engineering, vol. 7, no. 3, pp. 1508–1520, 2019.

[24] A. Bovet, J.-C. Delvenne, and R. Lambiotte, Flow stability for dynamic community detection, Science advances, vol. 8, no. 19, p. eabj3063, 2022.

[25] Y. Ai, X. Xie, and X. Ma, Graph contrastive learning for tracking dynamic communities in temporal networks, IEEE Transactions on Emerging Topics in Computational Intelligence, vol. 8, no. 5, pp. 3422–3435, 2024.

[26] L. Yu, P. Li, J. Zhang, and J. Kurths, Dynamic community discovery via common subspace projection, New Journal of Physics, vol. 23, no. 3, p. 033029, 2021.

[27] G. Rossetti and R. Cazabet, Community discovery in dynamic networks: a survey, ACM computing surveys (CSUR), vol. 51, no. 2, pp. 1–37, 2018.

[28] D. Zhuang, J. M. Chang, and M. Li, Dynamo: Dynamic community detection by incrementally maximizing modularity, IEEE Transactions on Knowledge and Data Engineering, vol. 33, no. 5, pp. 1934–1945, 2019.

[29] J. Jiang, S. Yao, Y. Chen, B. He, Y. Niu, Y. Li, S. Sun, and Y. Liu, Community detection in heterogeneous information networks without materialization, Proceedings of the ACM on Management of Data, vol. 3, no. 3, pp. 1–27, 2025.

[30] M. Seifikar, S. Farzi, and M. Barati, C-blondel: an efficient louvain-based dynamic community detection algorithm, IEEE Transactions on Computational Social Systems, vol. 7, no. 2, pp. 308–318, 2020.

[31] F. Liu, D. Choi, L. Xie, and K. Roeder, Global spectral clustering in dynamic networks, Proceedings of the National Academy of Sciences, vol. 115, no. 5, pp. 927–932, 2018.

[32] A. Failla, R. Cazabet, G. Rossetti, and S. Citraro, Describing group evolution in temporal data using multi-faceted events, Machine Learning, vol. 113, no. 10, pp. 7591–7615, 2024.

[33] N. İlhan and Ş. G. Öğüdücü, Predicting community evolution based on time series modeling, in 2015 IEEE/ACM International Conference on Advances in Social Networks Analysis and Mining (ASONAM). IEEE, 2015, pp. 1509–1516.

[34] Z. Dhouioui and J. Akaichi, Tracking dynamic community evolution in social networks, in 2014 IEEE/ACM International Conference on Advances in Social Networks Analysis and Mining (ASONAM 2014). IEEE, 2014, pp. 764–770.

[35] Y. Chi, X. Song, D. Zhou, K. Hino, and B. L. Tseng, On evolutionary spectral clustering, ACM Transactions on Knowledge Discovery from Data (TKDD), vol. 3, no. 4, pp. 1–30, 2009.

[36] F. Folino and C. Pizzuti, An evolutionary multiobjective approach for community discovery in dynamic networks, IEEE Transactions on Knowledge and Data Engineering, vol. 26, no. 8, pp. 1838–1852, 2013.

[37] P. Wang, L. Gao, and X. Ma, Dynamic community detection based on network structural perturbation and topological similarity, Journal of Statistical Mechanics: Theory and Experiment, vol. 2017, no. 1, p. 013401, 2017.

[38] M. Rosvall and C. T. Bergstrom, Mapping change in large networks, PloS one, vol. 5, no. 1, p. e8694, 2010.

[39] M. E. Newman and M. Girvan, Finding and evaluating community structure in networks, Physical review E, vol. 69, no. 2, p. 026113, 2004.

[40] J. Leskovec, J. Kleinberg, and C. Faloutsos, Graph evolution: Densification and shrinking diameters, ACM transactions on Knowledge Discovery from Data (TKDD), vol. 1, no. 1, pp. 2–es, 2007.

[41] A. Badalyan, N. Ruggeri, and C. De Bacco, Structure and inference in hypergraphs with node attributes, Nature Communications, vol. 15, no. 1, p. 7073, 2024.

[42] H. Qin, R.-H. Li, G. Wang, X. Huang, Y. Yuan, and J. X. Yu, Mining stable communities in temporal networks by density-based clustering, IEEE Transactions on Big Data, 2020.

[43] A. Lancichinetti, S. Fortunato, and F. Radicchi, Benchmark graphs for testing community detection algorithms, Physical review E, vol. 78, no. 4, p. 046110, 2008.

[44] M. E. Newman, Modularity and community structure in networks, Proceedings of the national academy of sciences, vol. 103, no. 23, pp. 8577–8582, 2006.

[45] W. M. Rand, Objective criteria for the evaluation of clustering methods, Journal of the American Statistical association, vol. 66, no. 336, pp. 846–850, 1971.

[46] A. R. Benson, D. F. Gleich, and J. Leskovec, Higher-order organization of complex networks, Science, vol. 353, no. 6295, pp. 163–166, 2016.

[47] L. Huang, C.-D. Wang, and H.-Y. Chao, Higher-order multi-layer community detection, in Proceedings of the AAAI Conference on Artificial Intelligence, vol. 33, no. 01, 2019, pp. 9945–9946.

[48] C. E. Tsourakakis, J. Pachocki, and M. Mitzenmacher, Scalable motif-aware graph clustering, in Proceedings of the 26th International Conference on World Wide Web, 2017, pp. 1451–1460.

[49] R. Milo, S. Shen-Orr, S. Itzkovitz, N. Kashtan, D. Chklovskii, and U. Alon, Network motifs: simple building blocks of complex networks, Science, vol. 298, no. 5594, pp. 824–827, 2002.

[50] N. K. Ahmed, J. Neville, R. A. Rossi, and N. Duffield, Efficient graphlet counting for large networks, in 2015 IEEE International Conference on Data Mining. IEEE, 2015, pp. 1–10.

[51] N. Pedreschi, D. Battaglia, and A. Barrat, The temporal rich club phenomenon, pp. 931–938, 2022.

[52] P. Jiao, T. Li, H. Wu, C.-D. Wang, D. He, and W. Wang, Hb-dsbm: Modeling the dynamic complex networks from community level to node level, IEEE Transactions on Neural Networks and Learning Systems, vol. 34, no. 11, pp. 8310–8323, 2022.

[53] E. K. Kao, S. T. Smith, and E. M. Airoldi, Hybrid mixed-membership blockmodel for inference on realistic network interactions, IEEE Transactions on Network Science and Engineering, vol. 6, no. 3, pp. 336–350, 2018.

[54] M. E. Newman, Assortative mixing in networks, Physical review letters, vol. 89, no. 20, p. 208701, 2002.

[55] H. Yin, A. R. Benson, and J. Leskovec, Higher-order clustering in networks, Physical Review E, vol. 97, no. 5, p. 052306, 2018.

Feiyu Yin received his M.Sc. degree from East China University of Science and Technology, Shanghai, China, in 2017. Currently, he is pursuing a Ph.D. degree at Fudan University. His research interests include computer science and deep learning.
https://orcid.org/0009-0001-8007-2199

Yu Xia received his Ph.D. degree in mechanical engineering from Chongqing University, Chongqing, China, in 2024. He is currently a Research Fellow in the State Key Laboratory of Mechanical System and Vibration, School of Mechanical Engineering, Shanghai Jiao Tong University, Shanghai, China. His research interests include prescribed performance control and electromechanical system control.
https://orcid.org/0009-0008-7271-5386

Agnieszka Siwocha received M.Sc. the degree from Lodz University of Technology, Faculty of Technical Physics, Computer Science and Applied Mathematics, and her a Ph.D. in 2015 in the fi eld of computer science, computer graphics at the University of Social Sciences, Łódź, Poland. She is currently an assistant professor at the Social Academy of Sciences in Łódź. She has a title of Adobe Certifi ed Expert, and provides training on Adobe software and computer graphics. Author of over 20 publications related to various problems of computer science, computer graphics and IT applications. Her present research interests include fractal coding, compression, and the quality of digital images, computer graphics, machine learning, and multifractal analysis.
https://orcid.org/0000-0003-2562-236X

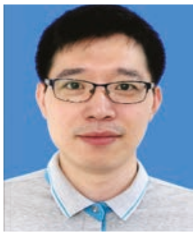

Zhanyu Cen received the B.S. degree in business administration from Sichuan Agricultural University in 2014. He currently serves as Deputy Chief Engineer at the Group Chief Engineer Office of Ningbo Zhongda Leader Intelligent Transmission Co., Ltd. His research focuses on the design and development of high-precision reducers/mechanisms, with particular expertise in innovative applications of bevel gears and hypoid gear technologies, while also dedicating efforts to the R&D of humanoid robot joint components and modules.
https://orcid.org/0009-0008-0066-3070

Jie Chen received the M.S. degree from the School of Automation, Central South University, Changsha, China, in 2018, and the Ph.D. degree from School of Information Science and Engineering, Fudan University, Shanghai, China, in 2023. He is currently a Research Associate Professor with the Department of Automation, University of Science and Technology of China, Hefei, China. His current research interests focus on multiagent collaborative control, game-theoretical optimization of complex networks, and reinforcement learning.
https://orcid.org/0000-0002-7335-995X